

## VIBRATION TESTS OF 1-STORY RESPONSE CONTROL SYSTEM USING INERTIAL MASS AND OPTIMIZED SOFTY SPRING AND VISCOUS ELEMENT

Kenji Saito<sup>1</sup>, Yoshifumi Sugimura<sup>2</sup>, Shigeki Nakaminami<sup>3</sup>, Hidenori Kida<sup>4</sup>, and Norio Inoue<sup>5</sup>

<sup>1</sup> Design Headquarters, NTT Facilities, INC., Dr. Eng.

<sup>2</sup> Research & Development Headquarters, NTT Facilities, INC.

<sup>3</sup> Technical Research Institute, Sumitomo Mitsui Construction Co., Ltd.

<sup>4</sup> Building Design Center, Sumitomo Mitsui Construction Co., Ltd.

<sup>5</sup> Professor, Graduate School of Tohoku University, Dr. Eng.

Email: [saitou23@ntt-f.co.jp](mailto:saitou23@ntt-f.co.jp)

### ABSTRACT :

The previous study have already proposed optimum response control method of 1-DOF system using linear viscous damper with rotational inertial mass and linear spring, and substituting equivalent linear Kelvin system for original system to develop simplified analysis and design procedures for practical applications. To achieve optimum control, we used the optimum design theory of the dynamic vibration absorber or the tuned-mass damper proposed by Den Hartog<sup>1)</sup>. In his theory, optimum design is achieved by minimizing the peaks of the resonance curve of the system. In this paper, we discuss proprieties of the optimum response control theory for magnification factor of displacement and acceleration. This paper also validated the tuning factor of substituting equivalent linear Kelvin system, and response damping ratio of the optimum control system subjected to random excitations.

**KEYWORDS:** Optimum response control, Passive control, Inertial mass, Viscous damping, Softy spring element, 1-Story system, Vibration tests

### 1. INTRODUCTION

In a system consisting of an inertial mass element  $m_r$  combined with a parallel-connected viscous element  $c_a$  and a series-connected softy spring element  $k_b$  (Figure 1(b)), the authors previously studied the enhancement of the energy-absorbing capacity of the viscous element achieved through appropriate synchronization between the natural circular frequency of the added component and that of the main component to produce dynamical expansion of the relative displacement of the viscous element, and theoretically proved the presence of an optimal damping and an optimal spring stiffness minimizing the peak of the resonant point of the main component for the given mass of the inertial mass element.<sup>2,3)</sup>

In the preceding report,<sup>4)</sup> the authors identified 3 different methods for optimum response control (ORC), including the control of the deformation response factor regarding the forced harmonic vibration directly acting on the mass  $m$  of the main component, as well as the control of the magnification factor of displacement and the control of the magnification factor of acceleration regarding the harmonic disturbance acting on the basal part of the system (there are referred to as deformation-, displacement-, and acceleration-based ORC, respectively, in this report for convenience's sake). We also demonstrated that the viscous coefficient  $c_a$  of the viscous element and the stiffness  $k_b$  of the spring element are determined uniquely by the mass ratio  $\mu$  between the mass of the inertial mass element  $m_r$  and the mass of the main component  $m$ . Furthermore, we proposed the substitution with an equivalent 1-DOF system based on the resonant frequency and the resonant damping factor of the system as a method for describing the effectiveness of the damping mechanism in the case of acceleration-based ORC, and found that the adjustment of stiffness and damping in this equivalent 1-DOF system might provide the possibility for prediction of the maximal response of the ORC system to random disturbances such as earthquake ground motions.

For the experiments reported here, we constructed a 1-story response control system with a linear viscous element, to be applied to displacement- and acceleration-based ORC methods among the 3 different methods

for ORC proposed by the authors.

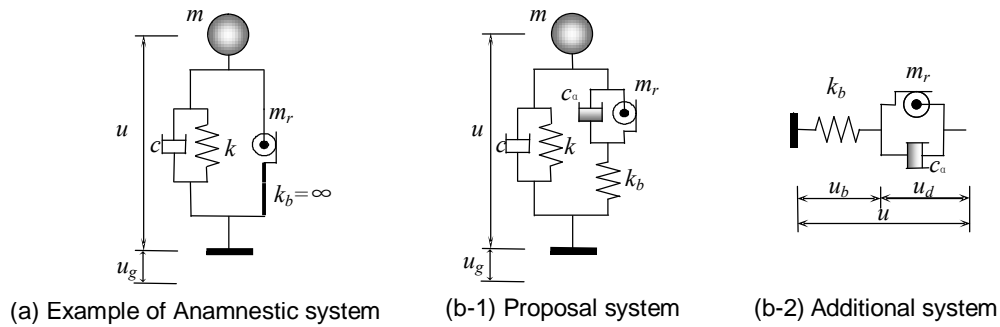


Figure 1. Single lumped mass system with inertial mass element

In this article, we test the validity of the theoretical solutions for ORC using the 2 different ORC systems constructed here, and describe the response characteristics of these systems under the influence of harmonic vibration and seismic wave vibration in comparison with the system in which the spring element is treated as a rigid body. In addition, we demonstrate the appropriateness of the method for adjusting stiffness and damping in the equivalent 1-DOF system, describe the result of accuracy verification for the mechanical model of this system according to time-history response analysis, and discuss the response-reduction effect of the ORC method on the main component under the influence of random disturbances such as seismic motions.

## 2. OPTIMUM RESPONSE CONTROL OF THE 1-DOF SYSTEM FOR THE PROPOSED SYSTEM

### 2.1 Response Magnification Factors of Proposed System

When the proposed system shown in Figure 1 is subjected to the ground acceleration  $\ddot{u}_g(t)$ , the equation of motion is:

$$m\ddot{u} + c\dot{u} + ku + f = -m\ddot{u}_g(t) \quad (2.1)$$

$$f = c_a\dot{u}_d + m_r\ddot{u}_d = k_b u_b \quad (2.2)$$

where  $m$  and  $m_r$  represent the main mass of the main component and the mass of the inertial mass element,  $k$  and  $k_b$  represent the stiffness of the main component and the stiffness of the series-connected spring element, and  $c$  and  $c_a$  represent the viscous coefficient of the main component and the viscous coefficient of the viscous element of the added component, respectively. In addition,  $\dot{u}_d$  and  $\ddot{u}_d$  represent the velocity and acceleration in the viscous element, respectively. In solving the above equation of motion, we define the following relationships:  $\omega_r^2 = k_b/m_r$ ,  $\omega_n^2 = k/m$ ,  $c/m = 2h_n\omega_n$ ,  $c_a/m_r = 2h_r\omega_r$ , where  $h_n$  and  $h_r$  represent the damping factor for the internal viscous damping in the main component and that for the viscous element in the added component, respectively, and  $\omega_r$  represents the natural circular frequency determined by the mass  $m_r$  of the inertial mass element and the stiffness  $k_b$  of the spring element (called hereinafter damper natural circular frequency).

### 2.2 ORC Method Using the Fixed Point Theory

Figure 2(a) shows the magnification factor of displacement at various values of the viscous coefficient of the viscous element ( $c_a=0, \hat{O}, 0.577, 0.475, 0.526 \text{ kN}\cdot\text{s}/\text{m}^3$ ), in which the mass ratio between the mass  $m_r$  of the inertial mass element and the main mass  $m$  of the system is  $\mu=0.25$ , the viscous coefficient of the main component is  $c=0$ , and the stiffness of the spring element is  $k_b=7.44 \text{ kN}/\text{m}$ . Figure 2(b) shows the magnification

factor of acceleration at various values of the viscous coefficient of the viscous element ( $c_a=0, \hat{O}, 0.278, 0.242, 0.260 \text{ kN}\cdot\text{s/m}$ )<sup>3)</sup>, in which the mass ratio is  $\mu=0.50$ , the viscous coefficient of the main component is  $c=0$ , and the stiffness of the spring element is  $k_b=3.08 \text{ kN/m}$ .

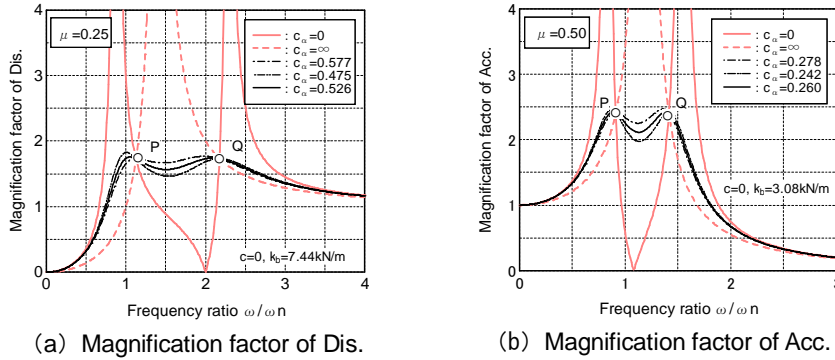


Figure 2. Magnification factor of system

As shown in Figure 2, when the viscous coefficient of the main component is set at  $c=0$ , the magnification factor of displacement and the magnification factor of acceleration in this system always have 2 fixed points P and Q, irrespective of the value of the viscous coefficient  $c_a$  of the viscous element.

Here, we use the fixed point theory,<sup>1)</sup> which was devised to determine the optimal values for stiffness and damping in a tuned mass damper (TMD), to derive the solutions under the condition giving the equal magnification factor at the fixed points P and Q (hereinafter called optimum synchronized frequency ratio) and under the condition giving the maximal magnification factor at the fixed points P and Q (hereinafter called optimum normalized relaxation time  $\lambda_{opt}$ ). A relationship  $\zeta_{opt}=\lambda_{opt}/2$  exists between the optimum normalized relaxation time  $\lambda_{opt}$  and the optimum damping factor  $\zeta_{opt}$  of the added component. We prefer to use the conversion from  $\lambda_{opt}$  to  $\zeta_{opt}$  in the following derivation of theoretical solutions.

The optimum synchronized frequency ratio  $\beta_{opt}$  and the optimum damping factor  $\zeta_{opt}$  are respectively represented by Eqn. 2.3 and Eqn. 2.4 for the magnification factor of displacement and Eqn. 2.5 and Eqn. 2.6 for the magnification factor of acceleration.<sup>3)</sup>

(i-1) Optimum synchronized frequency ratio for the magnification factor of displacement ( $\mu \leq 0.25$ ):

$${}_1\beta_{opt} = \frac{{}_1\omega_r}{\omega_n} = \frac{1 + \sqrt{1 - 4\mu}}{2\mu}, \quad {}_2\beta_{opt} = \frac{{}_2\omega_r}{\omega_n} = \frac{1 - \sqrt{1 - 4\mu}}{2\mu} \quad (2.3)$$

(i-2) Optimum damping factor for the magnification factor of displacement (added component):

$$\begin{cases} {}_1\zeta_{opt} = \sqrt{\frac{{}_1h_{r(P)}^2 + {}_1h_{r(Q)}^2}{2}} = \frac{\sqrt{3(1 + \sqrt{1 - 4\mu})}}{4} \\ {}_2\zeta_{opt} = \sqrt{\frac{{}_2h_{r(P)}^2 + {}_2h_{r(Q)}^2}{2}} = \frac{\sqrt{3(1 - \sqrt{1 - 4\mu})}}{4} \end{cases} \quad (2.4)$$

(ii-1) Optimum synchronized frequency ratio for the magnification factor of acceleration ( $\mu \leq 0.50$ ):

$$\beta_{opt} = \frac{\omega_r}{\omega_n} = \sqrt{\frac{2\mu - 1 + \sqrt{1 - 2\mu}}{\mu(1 - 2\mu)}} \quad (2.5)$$

(ii-2) Optimum damping factor for the magnification factor of acceleration (added component):

$$\zeta_{opt} = \sqrt{\frac{h_{r(P)}^2 + h_{r(Q)}^2}{2}} = \sqrt{\frac{3(1 - \sqrt{1 - 2\mu})}{8}} \quad (2.6)$$

Figure 3 shows the relationship between the optimum synchronized frequency ratio  $\beta_{opt}$  and the mass ratio  $\mu$  during ORC as the graphical representation of Eqn. 2.3 and Eqn. 2.5. Figure 4 shows the relationship between the optimum damping factor of the added component  $\zeta_{opt}$  and the mass ratio  $\mu$  during ORC as the graphical representation of Eqn. 2.4 and Eqn. 2.6. These Figures indicate that there are 2 optimal solutions in displacement-based ORC; and the optimum synchronized frequency ratio  $\beta_{opt}$  and the optimum damping factor  $\zeta_{opt}$  can be obtained only in the range of mass ratio  $\mu$  up to 0.25 in this case, and up to 0.5 in the case of acceleration-based ORC. Of the 2 solutions in displacement-based ORC, the one exceeding the  $\beta_{opt}$  value of 2 (designated  $1\beta_{opt}$ ) is a very special case involving extremely large viscous coefficient and stiffness, and therefore is excluded from further discussion.

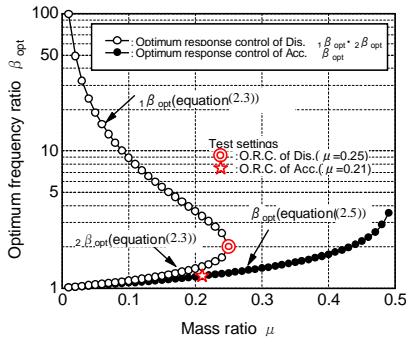


Figure 3. Optimum frequency ratio

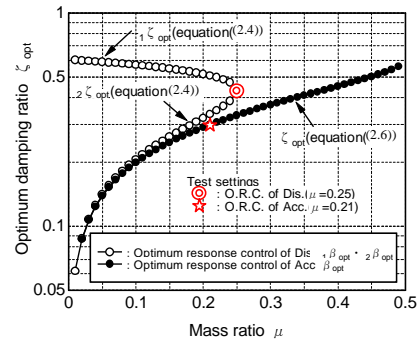


Figure 4. Optimum damping ratio (additional system)

The optimal viscous coefficient  $c_a$  for the viscous element and the optimal stiffness  $k_b$  for the spring element are represented by Eqn. 2.7 and Eqn. 2.8, using  $\beta_{opt}$  and  $\zeta_{opt}$ .

$$c = 2\zeta_{opt}\omega_r m_r \quad (2.7)$$

$$k_b = k(\beta_{opt})^2 \mu \quad (2.8)$$

### 3. DESCRIPTION OF TESTING SYSTEM

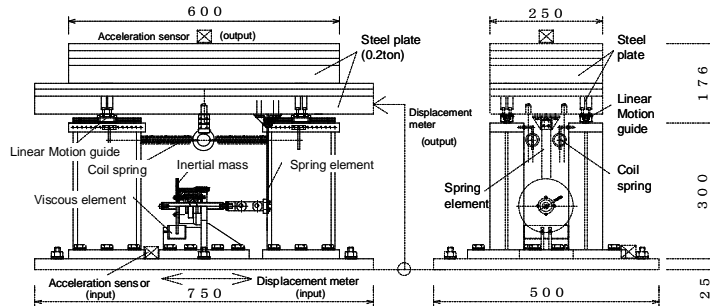
#### 3.1 System Overview

Table 1 summarizes the specifications for the test system. Figure 5 shows the detail drawing of the equipment. The main component of the testing system had the mass of  $m=0.2$  ton. The mass ratio was set at  $\mu=0.25$  for displacement-based ORC and  $\mu=0.21$  for acceleration-based ORC. The mass ratio for displacement-based ORC was the largest theoretical mass ratio, while that for acceleration-based ORC was the smallest mass ratio suitable to the addition of a viscous element in this experimental setting. Unless otherwise specified, displacement-based ORC and acceleration-based ORC are hereafter understood as implying the mass ratio of  $\mu=0.25$  and  $\mu=0.21$ , respectively. The optimum synchronized frequency ratio  $\beta_{opt}$  and the optimum damping factor  $\zeta_{opt}$  determined from the mass ratio during intended ORC are  $\beta_{opt}=2.00$  and  $\zeta_{opt}=0.431$  in displacement-based ORC and  $\beta_{opt}=1.23$  and  $\zeta_{opt}=0.301$  in acceleration-based ORC (marked in Figures 3 and 4). The optimal viscous coefficient  $c_a$  for the viscous element and the optimal stiffness  $k_b$  for the spring element, as determined from Eqn. 2.7 and Eqn. 2.8, are  $c_a=0.526$  kNs/m and  $k_b=7.44$  kN/m in displacement-based ORC and  $c_a=0.192$  kNs/m and  $k_b=2.39$  kN/m in acceleration-based ORC.

The system was composed of the main component, the inertial mass element, the viscous element, and the spring element. The main component was constructed so that a steel plate was attached atop four H-shaped steel pillars via linear motion guides (HSR12R1M+150LM), and four tension coil springs (diameter 3.5cm) connected the steel plate to the sides of the pillar tops. The main component was adjusted to have the natural period of  $T_n=1.0$  sec and the maximal vibration amplitude of  $\pm 50$  mm.

Table 1. Specification of testing system

Optimum response control (O.R.C.) method	Main mass	Equivalent mass	Mass ratio	Optimum frequency ratio	Optimum damping ratio	Coefficient of optimum viscous damping	Optimum spring constant
	m	mr	$\mu$	$\beta_{opt}$	$\zeta_{opt}$	C	kb
	ton	ton	—	—	—	kN·s/m	kN/m
Displacement	0.2	0.050	0.25	2.00	0.431	0.526	7.44
Acceleration	0.2	0.042	0.21	1.23	0.301	0.192	2.39



(a) Front elevation (b) Side elevation  
 Figure 5. System detail drawing

### 3.2 Inertial Mass Element, Viscous Element, and Spring Element

Table 2 summarizes the specifications for the inertial mass and viscous elements. Figure 6 shows the detailed drawing. The inertial mass element was a device utilizing the rotational inertial mass provided by a ball screw.<sup>5)</sup> The components consisted of the ball screw (WTF1530-2 +154LT), thrust bearings (model 6909), and weight disks attached to the nut (the rotating body). The setting of the mass ratio  $\mu$  was achieved by adding and reducing the number of weight disks.

Table 2. Specification of Inertial mass and viscous element

Constructional element	symbol	unit	Numeric		
			O.R.C.of Dis.	O.R.C.of Acc.	
Ball screw	Shaft diameter	DB	mm	15	
	Lead length	Ld	mm	30	
Rotating body (weight)	outer diameter	Do	mm	122	
	inside diameter	Di	mm	28	
	thickness	tr	mm	10	
	Mass	mi	ton	0.00079	0.00067
	Equivalent mass	mr	ton	0.050	0.042
Viscous fluid	Mass amplification	$\beta$	—	62.5	
	Viscosity(25°C)	$\eta_{25}$	cSt	Concoction 10000cSt and 30000cSt	Concoction 5000cSt and 10000cSt
	Velocity amplification	S	—	12.8	

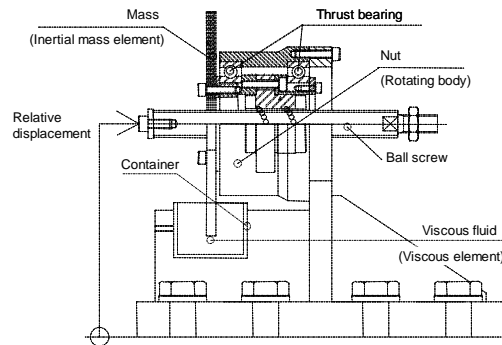


Figure 6. Inertial mass and viscous element detail drawing

## 4. DESCRIPTION OF EXPERIMENTS

As listed in Table 3, we conducted experiments in 3 cases: the main component only, displacement-based ORC, and acceleration-based ORC. Harmonic vibration tests and seismic vibration tests were conducted in each of these cases. Vibration was applied by placing the system on a shaking table and forcing horizontal vibration under displacement control. For each case, we also performed experiments without incorporating the viscous element ("no viscous element") and treating the spring element as a rigid body ("rigid spring element"), and compared the results with the response of the ORC system. The frequency of applied vibration was set in the range from 0.5 to 3 Hz with the frequency increments of 1/100 Hz at the maximum. Recording was continued until the response waveform attained a steady state, using the sampling frequency of 200 Hz. The input amplitude was adjusted so that the response displacement would be similar among different experimental cases, ensuring that the condition of the frictional force in the main component would be identical. The input



waveforms used in seismic vibration tests were BCJ-L2 and 4 actual seismic waves including El Centro-NS, Taft-EW, Hachinohe-NS, and JMA Kobe-NS.

Measurement points are shown in Figures 5 and 6. Measured parameters were the horizontal displacement and acceleration of the shaking table, the response displacement and response acceleration of the main component, the relative displacement of the inertial mass element or the viscous element, and the load on the added component. The load on the added component was measured with a 100-N load cell inserted between the clevis and the added component.

Table3. Cases of experiment

Cases of experiment	Mass ratio	Condition	Element type		
			Inertial mass ton	viscous kN·s/m	spring kN/m
Main frame only	—	—	—	—	—
Optimum response control (O.R.C) of Dis.	0.25	O.R.C	0.05	0.526	7.44
		Without viscous		$0.17^{-1}$	7.44
		Rigidity spring		0.526	$20^{+2}$
Optimum response control (O.R.C) of Acc.	0.21	O.R.C	0.042	0.192	2.39
		Without viscous		$0.12^{-1}$	2.39
		Rigidity spring		0.192	$20^{+2}$

\*1: Coefficient of equivalent viscous damping of device's friction \*2: Calculating from magnification factor

## 5. RESPONSE CHARACTERISTICS IN HARMONIC VIBRATION

### 5.1 Response Magnification Factor of ORC System

Figure 7 shows the response magnification factor during ORC in comparison with that of the "rigid spring element" case. The input amplitude was adjusted, for each frequency, to produce the response displacement within the range from  $u=5$  to 10 mm, and the response results are considered to include the contribution from the internal viscous damping in the main component ranging from  $h_n=0.03$  to 0.05. Solid lines represent the theoretical values for response magnification factor assuming that the internal viscous damping in the main component is  $h_n=0.04$  and other parameters were as specified in Table 3. Symbols represent experimental values. As seen in the Figure shows, the 2 peaks in experimental data during displacement-based ORC were shifted slightly to the high frequency end relative to theoretical curves. In addition, the experimental value for the response magnification factor during acceleration-based ORC was slightly higher than the theoretical value. However, generally good coincidence was observed regarding the response magnification factor during ORC, and acceleration response magnification factor.

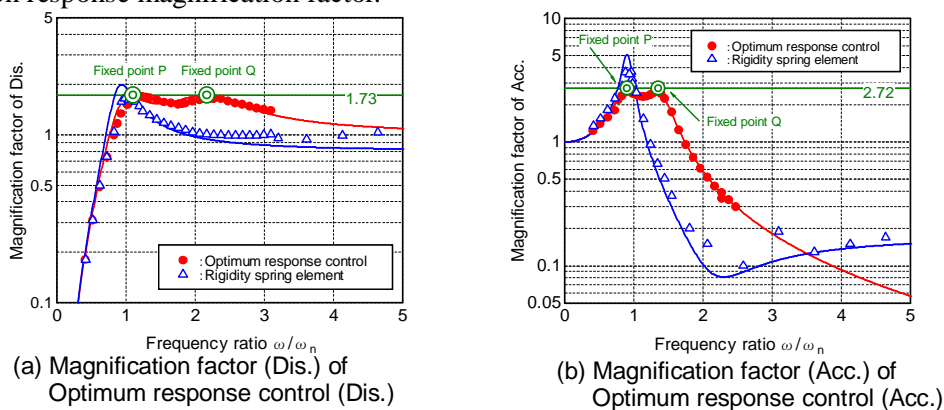


Figure7. Magnification factor of optimum response control system

### 5.2 Dynamic Characteristics of ORC System

#### 5.2.1 Replacement with Equivalent Kelvin Model

Next we consider the dynamic characteristics of the added component and the system using the replacement of ORC system with the equivalent Kelvin model. When the added component in Figure 8 is replaced with a

Kelvin model, the stiffness  $k_e(\omega)$  and the viscosity  $c_e(\omega)$  depend on the circular frequency of disturbance  $\omega$ , and are represented by Eqn. 5.1 and Eqn. 5.2, respectively.<sup>2)</sup>

$$k_e(\omega) = \frac{-m_r k_b^2 \omega^2 + m_r^2 k_b \omega^4 + c_a^2 k_b \omega^2}{(k_b - m_r \omega^2)^2 + (c_a \omega)^2} \quad (5.1)$$

$$c_e(\omega) = \frac{c_a k_b^2}{(k_b - m_r \omega^2)^2 + (c_a \omega)^2} \quad (5.2)$$

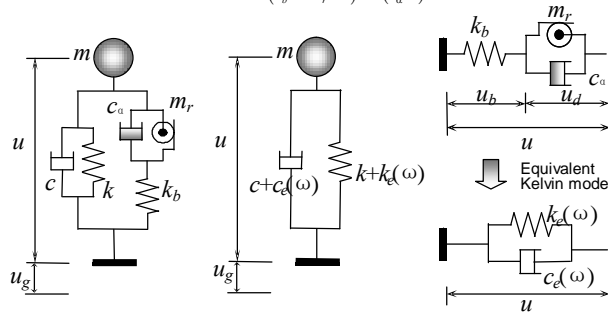


Figure8. Equivalent Kelvin replacement model

### 5.2.2 Equivalent Stiffness and Equivalent Viscous Coefficient of Added Component

Figure 9 shows the relationship between the equivalent stiffness  $k_e(\omega)$  and frequency ratio in the added component during acceleration-based ORC, as well as the relationship between the equivalent viscous coefficient  $c_e(\omega)$  and frequency ratio in the added component, in comparison with the "rigid spring element" case. Solid lines represent the theoretical values from Eqn. 5.1 and Eqn. 5.2, while symbols represent experimental values. In the 2 cases involving the softy spring element, experimental values were somewhat larger than theoretical values in the region of  $\omega/\omega_n \approx 1$ . This is considered to have resulted from the fact that the dynamic relative displacement of the viscous element diminishes in regions other than the vicinity of the optimum synchronized frequency ratio  $\beta_{opt}$ , and the friction of the ball screw becomes predominant in such regions. In other regions, the coincidence between experimental and theoretical values is relatively good.

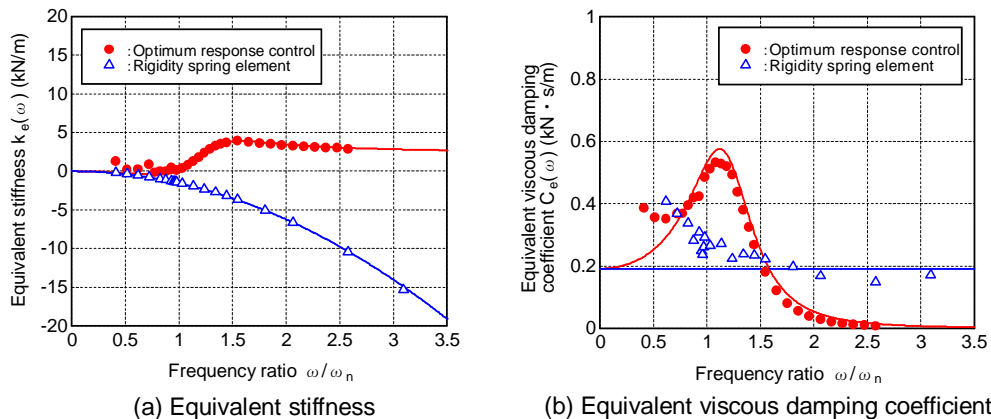


Figure9. Equivalent stiffness and Equivalent viscous damping coefficient of additional system in case of optimum response control of Acc.

## 6. RESPONSE CHARACTERISTICS IN SEISMIC VIBRATION

To test the validity of the analytical model for the added component (hereinafter called this equipment), we attempted to reproduce the response using the results from the tests with seismic wave input. The input waves were BCJ-L2 and the 4 samples of actual seismic waves described above. The primary natural period of the main component was set at 1.03 sec. Considering the response displacement of the system, the internal viscous damping in the main component was set at  $h_n=0.035$  for displacement-based ORC and  $h_n=0.025$  for acceleration-based ORC.

Table 4 lists the design parameters regarding the inertial mass element, the viscous element, and the friction element used in the analysis. As a typical example, Figure 10 shows the comparison between the analytical values and experimental values for acceleration-based ORC using the input of El Centro waves. Solid lines represent experimental values, and broken lines represent analytical values. Both hysteretic curves and time-history responses were sufficiently accurate even in the case of seismic waves containing various frequency components. The results for other wave samples were also similar.

Table4. Design parameter of analysis model

Element type	Design parameter	Symbol	Unit	Numeric	
				O.R.C. of Dis.	O.R.C. of Acc.
Inertial mass element	Shaft diameter of Ball screw	DB	mm	15	
	Lead length	Ld	mm	30	
	Outer diameter of Thrust bearing	DSB	mm	56.5	
	Outer diameter of Rotating body (mass)	D0	mm	103	
	Inside diameter of Rotating body (mass)	Di	mm	28	
	Mass of Rotating body	mi	ton	0.00079	0.00067
Viscous element	Effective length	Le	mm	10	
	Shear clearance	dy	mm	15	
	Viscosity (25°C)	25	cSt	3500	1600
	Repeated dependent coefficient (R.D.C.)			1	
	Vibration frequency for R.D.C.	f	Hz	1.03	
	Design temperature	T	°C	20	
Friction element	Friction coefficient of Ball screw	B		0.005	
	Friction coefficient of Thrust bearing	SB		0.0078	
	Frictional force per unit length	Qsi	kN	0.000008	

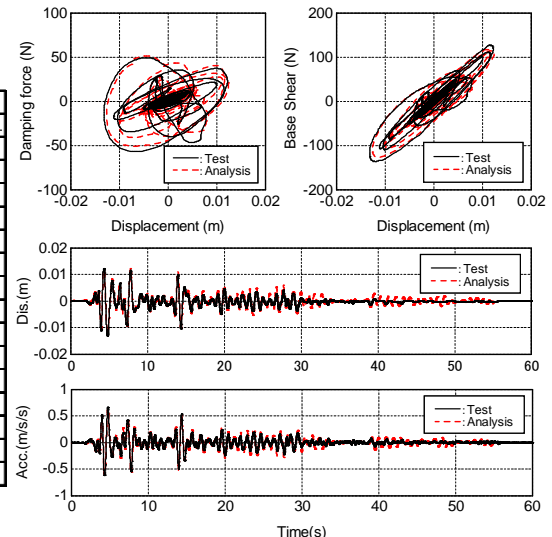


Figure10. Analysis Value and experimental value comparison in case of O.R.C of Acc. (El Centro-NS)

## 7. SUMMARY AND CONCLUSIONS

In this study, we conducted vibration experiments on the 1-story system consisting of an inertial mass element, an optimized softy spring element, and a viscous element to test the validity of the theoretical values regarding the displacement-based ORC and acceleration-based ORC proposed by us. We also examined the dynamic characteristics of this system. The following summarizes our conclusions.

- (1) Displacement-based ORC and acceleration-based ORC during harmonic vibration acting on the basal part of our proposed system can minimize the peak of the resonance point of the main component.
- (2) By appropriately synchronizing the inertial mass element and the softy spring element with the natural circular frequency of the main component, it is possible to increase the dynamic deformation of the viscous element and enhance the damping effect of the viscous element.
- (3) The result of the time-history analysis of the ORC system incorporating the analytical model of this equipment shows relatively good coincidence with experimental values.

## REFERENCES

- 1) J. P. Den Hartog. Mechanical Vibrations, 4<sup>th</sup>ed., Dover, New York, 1985.
- 2) Saito, K., Kurita, S. and Inoue, N. (2007). Optimum Response Control of 1-DOF System Using Linear Viscous Damper with Inertial Mass and Its Kelvin-type Modeling. *Journal of Structural Engineering*, Vol.53B, 53-66.
- 3) Saito, K., Nakaminami, S., Kida, H. and Inoue, N. (2008). Vibration Tests of 1-story Response Control System Using Inertial Mass and Optimized Softy Spring and Viscous Element. *Journal of Structural Engineering*, Vol.54B, 623-634.
- 4) Saito, K., Sugimura, Y. and Inoue, N. (2004). A Study on Response Control of a Structure Using Viscous Damper with Inertial Mass. *Journal of Structural Engineering*, Vol.54B, 635-648.
- 5) Nakaminami, S. et al. (2005). Development of Viscous Damping Device with Inertial Mass Element, Reports of Technical Research Institute of Sumitomo Mitsui Construction Co., Ltd. No.3.